HHS Public Access

Author manuscript

Sci Signal. Author manuscript; available in PMC 2020 March 10.

Published in final edited form as:

Sci Signal. ; 12(598): . doi:10.1126/scisignal.aap7336.

Inflammation induces stress erythropoiesis through heme-dependent activation of SPI-C

Laura F. Bennett[1,2], **Chang Liao**[2,3,4,*], **Michael D. Quickel**[2,3,5], **Beng San Yeoh**[6,†], **Matam Vijay-Kumar**[4,6,7,†], **Pamela Hankey-Giblin**[1,2,3,4], **K. Sandeep Prabhu**[2,3,4,6], **Robert F. Paulson**[1,2,4,6,‡]

[1]Intercoiiege Graduate Program in Genetics, Penn State University, University Park, PA 16802, USA.

[2]Department of Veterinary and Biomedical Sciences, Penn State University, University Park, PA 16802, USA.

[3]Graduate Program in Pathobiology, Penn State University, University Park, PA 16802, USA.

[4]Center for Molecular immunology and infectious Disease, Penn State University, University Park, PA 16802, USA.

[5]Clinical and Translational Science institute, Penn State College of Medicine, Her- shey, PA 17033, USA.

[6]Graduate Program in Molecular, Cellular and integrative Biosciences, Penn State University, University Park, PA 16802, USA.

[7]Department of Nutritional Sciences, Penn State University, University Park, PA 16802, USA.

Abstract

Inflammation alters bone marrow hematopoiesis to favor the production of innate immune effector cells at the expense of lymphoid cells and erythrocytes. Furthermore, proinflammatory cytokines inhibit steady-state erythropoiesis, which leads to the development of anemia in diseases with chronic inflammation. Acute anemia or hypoxic stress induces stress erythropoiesis, which generates a wave of new erythrocytes to maintain erythroid homeostasis until steady-state erythropoiesis can resume. Although hypoxia-dependent signaling is a key component of stress erythropoiesis, we found that inflammation also induced stress erythropoiesis in the absence of

‡Corresponding author. rfp5@psu.edu.

*Present address: Department of Medicine, University California, San Francisco, San Francisco, CA 94143, USA.

†Present address: Department of Physiology and Pharmacology, University of, Toledo College of Medicine and Life Sciences, Toledo, OH 43614, USA.

Author contributions: L.F.B., M.D.Q., C.L., and R.F.P. designed experiments and analyzed the data. L.F.B., M.D.Q., C.L., and B.S.Y. performed the experiments. L.F.B. and R.F.P. wrote the manuscript. M.V.-K., K.S.P., and P.H.-G. helped plan experiments and provided comments on the manuscript.

Competing interests: R.F.P. is a consultant with Rubius Therapeutics. The other authors declare that they have no competing interests.

Data and materials availability: All data needed to evaluate the conclusions in the paper are present in the paper or in the Supplementary Materials.

SUPPLEMENTARY MATERIALS

stke.sciencemag.org/cgi/content/full/12/598/eaap7336/DC1

hypoxia. Using a mouse model of sterile inflammation, we demonstrated that signaling through Toll-like receptors (TLRs) paradoxically increased the phagocytosis of erythrocytes (erythrophagocytosis) by macrophages in the spleen, which enabled expression of the heme-responsive gene encoding the transcription factor SPI-C. Increased amounts of SPI-C coupled with TLR signaling promoted the expression of *Gdf15* and *Bmp4*, both of which encode ligands that initiate the expansion of stress erythroid progenitors (SEPs) in the spleen. Furthermore, despite their inhibition of steady-state erythropoiesis in the bone marrow, the proinflammatory cytokines TNF-α and IL-1β promoted the expansion and differentiation of SEPs in the spleen. These data suggest that inflammatory signals induce stress erythropoiesis to maintain erythroid homeostasis when inflammation inhibits steady-state erythropoiesis.

INTRODUCTION

Anemia of inflammation (AI) is common among patients with persistent inflammatory conditions, such as chronic infections, cancer, and autoimmune disorders (1–4). These conditions are characterized by the overproduction of proinflammatory cytokines, and many proinflammatory cytokines are known to inhibit steady-state bone marrow erythropoiesis. In particular, tumor necrosis factor-α (TNF-α) and interferon-γ (IFN-γ) inhibit the growth and differentiation of erythroid progenitors in the bone marrow as well as shorten the life span of mature circulating erythrocytes (5–11). In addition to direct inhibition of bone marrow erythropoiesis during inflammation and infection, inflammatory cytokines shift hematopoiesis toward the production of myeloid cells. Stimulation of Toll-like receptors (TLRs) on hematopoietic stem cells (HSCs) results in increased monocyte and macrophage production and a loss of lymphoid potential (12). Interleukin-1 (IL-1) has also been shown to inhibit lymphopoiesis and erythropoiesis, and chronic exposure to IL-1 drives HSCs toward myelopoiesis (13). In addition, the proinflammatory cytokine IL-6 induces expression of hepcidin mRNA (*hamp1*), resulting in decreased iron availability and iron-restricted erythropoiesis (14,15).

Stress erythropoiesis is a stress response pathway capable of rapidly producing large numbers of mature erythrocytes during acute anemia when steady-state production is not sufficient to correct the anemia. It is best understood in mice where it occurs primarily in the adult spleen and liver and relies on unique signals from the microenvironment that are distinct from the signals involved in steady-state erythropoiesis (16–20). Furthermore, stress erythroid progenitors (SEPs) are derived directly from short-term reconstituting HSCs ($CD34^+Kit^+Sca1^+Lin^-$), which migrate from the bone marrow to the spleen, where hedgehog (HH) and bone morphogenetic protein 4 (BMP4) signaling specify them as SEPs (16, 19, 20). Early SEPs can be divided into three distinct populations: $CD34^+CD133^+Kit^+Sca1^+$, $CD34^-CD133^+Kit^+Sca1^+$, and $CD34^-CD133^-Kit^+Sca1^+$. Each of these populations is transplantable and self-renewing, but despite their stem cell markers, they are erythroid restricted (16, 20). In addition to HH and BMP4, growth and differentiation factor 15 (GDF15) is a critical regulator of the expansion of SEPs, and the absence of any of these signals results in a reduction in stress erythroid potential (20). The development of SEPs proceeds through three phases, the first of which is the expansion of the early SEP progenitor populations. At this point, the ability of SEPs to differentiate is limited. The rise

in serum erythropoietin (EPO) and tissue hypoxia promotes a transition where signals in the spleen change, and the SEPs acquire the ability to differentiate. In the final phase, SEPs synchronously differentiate to generate a wave of new erythrocytes (20). All these signals work in concert to tightly regulate the expansion and differentiation of SEPs and ensure that the pathway is only activated in times of need.

The induction of inflammation with heat-killed *Brucella abortus* reduces steady-state erythropoiesis in the bone marrow and causes an expansion of erythroid progenitors in the spleen, suggesting that SEPs differ from steady-state progenitors in their responses to inflammatory stimuli (14, 21, 22). Mice infected with *Salmonella* or murine *Plasmodium* strains also show a large expansion of the erythroid population in the spleen after infection (23–25). Activation of TLR2 with the fungal β-glucan zymosan A results in an increase in stress erythroid burst-forming units (BFU-Es), and, unlike bone marrow erythroid progenitors, stress BFU-E production is not inhibited by IFN-γ (26). However, details about the mechanisms that regulate the proliferation of SEPs during inflammation and how they are affected by proinflammatory cytokines are not well understood.

Tissue hypoxia plays a key role in inducing the expression of *Bmp4* and in promoting the response of SEPs to different signals during the recovery from anemia (20, 27). Although hypoxia is a critical aspect of stress erythropoiesis, here, we describe a mechanism by which inflammation induces stress erythropoiesis in the absence of anemic or hypoxic stress. We demonstrate that activation of TLR2 by zymosan A resulted in an increase in erythrophagocytosis, which induces a signaling cascade that led to the expression of *Gdf15* and *Bmp4* and the activation of the stress erythropoiesis pathway. This response occurred rapidly and in the absence of anemia. Increased erythrophagocytosis led to an increase in intracellular heme caused by the breakdown of hemoglobin. This increase in heme in turn promoted the induction of *Spic*, which encodes the heme-regulated transcription factor SPI-C (28). Our data show that SPI-C and TLR activation play a critical role in inducing stress erythropoiesis during inflammation. In addition to inducing erythrophagocytosis, inflammation also induced the production of proinflammatory cytokines, which others have shown to inhibit bone marrow steady-state erythropoiesis. In contrast to steady-state erythropoiesis, we show that the proinflammatory cytokine TNF-α and, to a lesser extent, IL-1β enhanced stress erythropoiesis in vitro in murine bone marrow cultures. Together, these data demonstrate that inflammation induces stress erythropoiesis to offset inhibition of steady-state erythropoiesis and maintain erythroid homeostasis.

RESULTS

Inflammatory stimulation rapidly induces stress erythropoiesis

We used a mouse model of sterile inflammation in which priming with bacterial lipopolysaccharide (LPS), which stimulates TLR4, was followed by treatment with the TLR2 ligand zymosan A. This regimen induces an acute peritonitis that persists for about 48 to 72 hours before resolving into a chronic inflammatory disease from day 5 onward (Fig. 1A) (26, 29). The mice develop anemia within 7 to 9 days after zymosan treatment, which resolves into a periodic anemia (fig. S4). Injection with EPO can partially correct the low hemoglobin and erythrocyte numbers in the anemic mice; however, this effect is not due to

increased bone marrow erythropoiesis but rather an induction of stress erythropoiesis in the spleen (26). Although it is not unexpected that inducing stress erythropoiesis improves zymosan-induced anemia, it remained unclear why endogenous stress erythropoiesis failed to prevent the initial development of anemia. To address this question, we assayed for stress erythropoiesis in mice treated with LPS and zymosan.

Activation of the BMP4-dependent stress erythropoiesis pathway by acute anemic stress is characterized by an expansion of stress BFU-Es in the spleen, and hypoxia plays a role in initiating this response. Zymosan-treated mice do not develop anemia until 7 to 9 days after treatment (26, 29). Despite the lack of anemia, we observed a significant increase in the number of stress BFU-Es in the spleen between 24 and 72 hours after zymosan treatment (Fig. 1B). Analysis of SEP populations by flow cytometry revealed a large expansion of $CD34^+CD133^+Kit^+Sca1^+$ cells, the most immature subset of the SEPs (Fig. 1C and fig. S1A) (20). In response to EPO, this population of $CD34^+CD133^+Kit^+Sca1^+$ cells differentiates into $CD34^-CD133^-Kit^+Sca1^-CD71^+Ter119^{lo}$ stress BFU-Es (16, 20). These data demonstrate that zymosan-induced inflammation triggered an immediate expansion of early SEPs that develop into stress BFU-Es. In the bone marrow, BFU-Es decreased within 36 hours after treatment with zymosan (fig. S1B). This is consistent with the findings from Millot *et al*. showing a decrease in both $Ter119^+$ cells in the bone marrow and reduced numbers of immature erythrocytes after treating with zymosan (26).

GDF15 and BMP4 drive the proliferation of SEPs and their differentiation into stress BFU-Es. Treatment with zymosan leads to increased mRNA expression of both of these essential factors within the first 9 hours after treatment. *Gdf15* expression in the spleen increased more than 20-fold 3 hours after zymosan treatment (Fig. 1D), and *Bmp4* expression in the spleen increased 12-fold at 9 hours after treatment (Fig. 1E). We previously demonstrated that hypoxia stimulates *Bmp4* expression in the spleen. However, the rapid increase in *Bmp4* mRNA after zymosan treatment occurred well before the onset of anemia, which suggests that mechanisms other than hypoxia stimulate *Bmp4* expression in response to inflammation.

The expansion of stress BFU-Es requires BMP4- and GDF15-dependent signaling. *flexed-tail* (*f/f*) mice exhibit a delayed stress erythropoiesis response due to a splicing mutation in *Smad5*, resulting in insufficient BMP4 signaling during stress erythropoiesis (17, 30). In response to zymosan treatment, *f/f* mice exhibited a similar delay in stress erythropoiesis. At 36 hours, *f/f* mice had significantly fewer stress BFU-Es compared to wild-type mice, but by 72 hours, the number of stress BFU-Es was comparable to wild type (Fig. 1F). GDF15 is also required for the expansion of SEPs. $Gdf15^{-/-}$ mice failed to expand the population of stress BFU-Es in the spleen and generated significantly fewer colony-forming BFU-Es than did wild-type mice at 36 and 72 hours after inducing inflammation (Fig. 1F). In addition to the defects in SEP expansion, both mutant strains exhibited significant lethality in the first 4 days after treatment, with $Gdf15^{-/-}$ mice exhibiting 90% lethality compared to 40 and 10% for *f/f* and wild-type mice, respectively (fig. S1C).

In addition to the increased expression of *Gdf15* and *Bmp4* in the spleen, stress erythropoiesis also requires high amounts of serum EPO to promote the transition of SEPs

from a state of self-renewal to differentiation (20). EPO is produced in the kidney, where expression of *Epo* is regulated by the hypoxia-inducible factor 2α (HIF-2α) (31). Under normoxic conditions, a von Hippel-Lindau–dependent ubiquitin ligase promotes the degradation of HIF-2α (32). Despite the lack of anemia, we observed an accumulation of HIF-2α protein in the kidney after treatment with zymosan, peaking at 9 hours (Fig. 1G). This increase in HIF-2α protein was followed by an about 30-fold increase in *Epo* expression at 24 hours after treatment, and a corresponding rise in serum EPO concentration was observed at 24 and 36 hours (Fig. 1H). This increase in serum EPO is sufficient to activate stress erythropoiesis and is similar to what we observe during the recovery from bone marrow transplant (16, 20). These data demonstrate that treatment with zymosan induces the expression of key signals that are required for the expansion and differentiation of SEPs.

Stress erythropoiesis generates new erythrocytes immediately after zymosan treatment, delaying the onset of anemia

Reticulocyte numbers dropped steadily on days 2 and 4 after zymosan treatment, consistent with an inhibition of bone marrow erythropoiesis, before increasing on day 6 and continuing to rise steadily through day 14 after the burst of stress erythropoiesis in the spleen (Fig. 2A). There was no change in the number of reticulocytes in phosphate-buffered saline (PBS)–treated controls (Fig. 2A). BFU-Es in the spleen increased between days 0 and 6 after treatment with zymosan, and the rise in reticulocytes followed this increase (Fig. 2B). BFU-Es represent the earliest cells committed to the erythroid fate, and the lag between increased BFU-Es and the rise in reticulocytes is consistent with time required for maturation in vivo. In *f/f* mice, there is a lag in the increase in reticulocytes, and their numbers are statistically significantly lower than those in wild-type mice on days 6 and 8. However, reticulocytes began to increase on day 10 and reached wild-type numbers by day 14 (Fig. 2C). We also analyzed erythrocyte turnover by biotinylating erythrocytes in vivo. Over a 14-day period after zymosan treatment, we observed a small but significant increase in erythrocyte turnover in wild-type mice compared to PBS-treated controls (Fig. 2D). *f/f* mice exhibited a significantly higher percentage of biotinylated erythrocytes than their wild-type counterparts from days 6 to 14 after zymosan treatment, suggesting that fewer new erythrocytes had entered circulation (Fig. 2E). Hematocrits for wild-type and *f/f* mice decrease steadily over the first 4 days after treatment. However, between days 6 and 8, *f/f* mice exhibited a rapid drop in hematocrit, whereas wild-type mice showed a more modest drop (Fig. 2F). Hematocrit values seemed to increase slightly on day 10, consistent with the corresponding increase in reticulocytes on that day, before dropping again and reaching a lower nadir than in wild-type mice. Together, these data suggest that activation of the stress erythropoiesis pathway by inflammation increases reticulocyte production, and this influx of new erythrocytes into circulation acts to maintain hematocrit values temporarily. In the case *of f/f* mice, in which induction of stress erythropoiesis is delayed, hematocrit values dropped rapidly and remained lower than those of wild-type mice.

Zymosan induces *GDF15* expression by increasing erythrophagocytosis by splenic macrophages

Although the wild-type mice were not anemic in the first 48 to 72 hours after zymosan treatment, they exhibited all the hallmarks of activating stress erythropoiesis, suggesting that inflammatory signals are capable of inducing stress erythropoiesis through a previously unrecognized hypoxia-independent mechanism. The initial feature of this response was the increase in *Gdf15* expression in the spleen. Two mechanisms are known to stimulate *Gdf15* expression. One is the heme-dependent activation of the transcription factor SPI-C, and the second is the TLR-dependent activation of nuclear factor κB (NF-κB) (28, 33). *Spic* mRNA expression is repressed by the BTB domain and CNC homology 1 (BACH1) protein, but BACH1 is degraded in the presence of heme, leading to increased *Spic* expression (34–36). This heme-dependent signal is required for the development of splenic red pulp macrophages and bone marrow macrophages (28, 37). Erythrophagocytosis by red pulp macrophages plays a key role in maintaining erythroid homeostasis. Previous work from our laboratory showed that erythrophagocytosis by red pulp macrophages in the spleen is associated with increased production of the chemokine CCL2, which recruits monocytes to the spleen to establish the niche for stress erythropoiesis after bone marrow transplant (38). Signal regulatory protein alpha (SIRPα) is present on the surface of macrophages and negatively regulates erythrophagocytosis by binding to CD47 on the surface of erythrocytes. This interaction acts as a “don’t-eat-me” signal (39–41). As red blood cells (RBCs) age, the abundance of CD47 on the cell surface decreases, resulting in less interaction with macrophage SIRPα and leading to phagocytosis of the erythrocyte (39). Mutation of SIRPα leads to shorter erythrocyte half-life and a mild anemia that is compensated by stress erythropoiesis in the spleen (42). Activation of TLRs decreases surface abundance of SIRPα (40). In addition, TLR signaling promotes erythrophagocytosis through the spleen tyrosine kinase (Syk)– and phosphatidylinositol 3-kinase (PI3K)–dependent signaling pathways independently of CD47 and SIRPα (42). We propose that TLR signaling decreases the amount of Sirpα on macrophage plasma membranes and, in concert with Syk and PI3K signals, increases erythrophagocytosis. The subsequent turnover of hemoglobin releases heme, driving increased expression of *Spic* and leading to the expression of *Gdf15*. Because of the rapid increase in *Gdf15* expression in the spleen after treatment with zymosan, we tested whether zymosan can induce heme-dependent signaling in splenic macrophages and focused our studies on the events occurring within the first 3 hours after zymosan treatment.

We first examined SIRPα protein on the surface of $F4/80^+$ cells (macrophages) isolated from the spleen by flow cytometry immediately after treatment with zymosan. SIRPα surface abundance decreased significantly by 150 min after zymosan treatment, resulting in a relative loss of 10.7% of SIRPα compared to unstimulated controls (Fig. 3A). To address whether this small reduction in SIRPα on the surface of macrophages was capable of increasing phagocytosis of circulating erythrocytes, we measured erythrocyte uptake by splenic macrophages. Erythrocytes were labeled with carboxyfluorescein diacetate succinimidyl ester (CFSE) and transfused into LPS-treated mice such that they constituted about 5 to 10% of the circulating erythrocytes (Fig. 3B). We observed no significant difference in the percentage of $CFSE^+$ cells in the blood of PBS- or zymosan-treated mice at 3 hours after treatment, demonstrating that $CFSE^+$ and $CFSE^-$ erythrocytes were

phagocytosed at equal rates (Fig. 3C). However, examination of F4/80$^+$ phagocytes in the spleens revealed that there was a small but significant increase in the percentage of macrophages that had phagocytosed CFSE$^+$ erythrocytes (F4/80$^+$CFSE$^+$ cells) in zymosan-treated mice, indicating a small increase in erythrophagocytosis that was detectable at 3 hours after treatment with zymosan (Fig. 3C). Twenty-four hours after treatment, F4/80$^+$CFSE$^+$ cells in the spleens of zymosan-treated mice continued to increase after treatment compared to PBS-treated mice (Fig. 3D). At no time was there a significant change in the percentage of CFSE$^+$ erythrocytes in the blood (Fig. 3D).

The breakdown of hemoglobin from phagocytosed erythrocytes releases free heme, which can be toxic to the cell. We observed that, after zymosan treatment, the expression of *heme oxygenase 1* (*Hmox1*), which encodes an enzyme that breaks down heme, was induced at 60 min after treatment (Fig. 4A). *Feline leukemia virus subgroup C cellular receptor 1* (*Flvcr*), which encodes the heme exporter (43), was also induced at later time points (Fig. 4B). These data indicate that the concentration of intracellular heme increased in the spleen after zymosan treatment. We examined expression of *Spic*, which is known to promote the differentiation of monocytes into mature red pulp macrophages. *Spic* expression is normally repressed by the transcriptional repressor BACH1, which is negatively regulated by heme (28). After treatment with zymosan, *Spic* expression was significantly increased at 90 min with a peak increase at 150 min (Fig. 4C). BACH1 protein abundance, as measured by Western blot, also decreased rapidly after treating with zymosan (Fig. 4D). To determine whether changes in heme-regulated genes were occurring primarily in macrophages that have phagocytosed CFSE$^+$ erythrocytes, we sorted F4/80$^+$CFSE$^-$ and F4/80$^+$CFSE$^+$ cells by flow cytometry. The increased expression of *Spic* was limited to CFSE$^+$ macrophages, implying that heme derived from erythrophagocytosis led to increased *Spic* expression (Fig. 4E). Similarly, the expression of *Gdf15* was significantly increased by 3000-fold but only in F4/80$^+$CFSE$^+$ macrophages (Fig. 4F). Both F4/80$^+$CFSE$^-$ and F4/80$^+$CFSE$^+$ cells sorted from PBS-treated mice had significantly lower expression of *Gdf15* and *Spic* when compared with the expression of these genes in F4/80$^+$CFSE$^+$ cells from zymosan-treated mice (fig. S2, A and B). Together, these data are consistent with a mechanism wherein zymosan treatment increases erythrophagocytosis, resulting in increased abundance of intracellular free heme, which is sufficient to drive the expression of heme-related genes and, in particular, lead to SPI-C–dependent induction of *Gdf15*.

At baseline, mice with mutations in CD47 or SIRPα exhibit faster erythrocyte turnover than control mice and exhibit mild splenomegaly (42). However, when treated with inflammatory stimuli such as LPS, *CD47*$^{-/-}$ and *Sirpa*$^{-/-}$ mice exhibit an exaggerated response characterized by excessive erythrophagocytosis, splenomegaly, and anemia, which is not observed in wild-type animals (42). The more potent erythrophagocytosis in both *CD47*$^{-/-}$ and *Sirpa*$^{-/-}$ mice suggests that the CD47-Sirpα signaling axis is critically important for negatively regulating erythrophagocytosis in response to inflammation. Increased erythrophagocytosis in response to LPS or other inflammatory stimuli in the mutant mice could be abolished in the presence of inhibitors of either Syk or PI3K (42). We stimulated bone marrow–derived macrophages (BMDMs) with zymosan alone or zymosan and either the PI3K inhibitor LY294002 or the Syk inhibitor piceatannol. SIRPα surface abundance decreased significantly after treatment with zymosan, even in the presence of LY294002 or

piceatannol (Fig. 4G). Erythrophagocytosis was significantly increased after treatment with zymosan, and *Gdf15* mRNA expression was also increased, as observed in vivo (Fig. 4, H and I). Both piceatannol and LY294002 inhibited erythrophagocytosis and the increase in *Gdf15* expression (Fig. 4, H and I). These data support the conclusion that TLR signaling decreases the production of SIRPα, which negatively regulates erythrophagocytosis and promotes the phagocytosis of erythrocytes through a PI3K- and Syk-dependent pathway that in turn drives an increase in *Gdf15* expression.

TLR2-dependent signaling contributes to the increase in *Spic* and *GDF15* expression after zymosan treatment

MyD88 is a critical adaptor protein for signaling through all TLRs except TLR3 (44, 45). Previous work showed that *Salmonella* infection increases the number of $TER119^+CD71^+$ erythroid progenitors in the spleen in wild-type mice but not in MyD88-deficient mice ($MyD88^{-/-}$) (25). These data suggest that increase in splenic stress erythropoiesis by inflammatory stimuli is a MyD88-dependent event. To determine whether the response to zymosan was MyD88 dependent, we used either wild-type or $MyD88^{-/-}$ BMDMs to assess the role of MyD88 in regulating erythrophagocytosis and the increase in the expression of *Spic* and *Gdf15*. $MyD88^{-/-}$ mutant BMDMs failed to decrease SIRPα cell surface abundance after treatment with zymosan (Fig. 5A). Furthermore, the mutant macrophages exhibited significantly less phagocytosis of CFSE-labeled erythrocytes (Fig. 5B). Their inability to phagocytose erythrocytes led to a weak increase in *Spic* expression, which was lower than the amount of *Spic* expression induced in wild-type BMDMs (Fig. 5C). The lack of robust *Spic* expression prevented the increase in *Gdf15* expression in $MyD88^{-/-}$ BMDMs (Fig. 5D).

Because NF-κB has been shown to induce the expression of *Gdf15* (33), SPI-C and NF-κB could work in concert to stimulate *Gdf15* expression. We isolated primary adherent cells from the spleen, about 12 to 14% of which were $F4/80^+$, and treated them in vitro with either zymosan or aged erythrocytes. Both zymosan and aged erythrocytes were capable of increasing *Spic* and *Gdf15* expression in the cells, but treatment with zymosan produced the greatest increase in *Spic* and *Gdf15* mRNA expression (Fig. 5, E and F). Inhibition of NF-κB by JSH-23 did not affect the induction in *Gdf15* or *Spic* mRNA expression in zymosan-treated cells or in the cells incubated with aged erythrocytes (Fig. 5, E and F). These data demonstrate that TLR-dependent signaling plays a role in the initiation of stress erythropoiesis, but NF-κB–dependent regulation of *Gdf15* expression is not involved in this context.

The increase in *Gdf15* expression was transient. EPO can act on macrophages where its effects are anti-inflammatory (46). We observed that EPO treatment also decreased the induction of *Spic* and *Gdf15* expression in cells stimulated with zymosan (Fig. 5, E and F). Analysis of serum EPO abundance showed a smaller increase in EPO at 3 hours followed by a much larger increase in starting at 12 hours after treatment (Fig. 1H). This early increase in EPO, coupled with an increase in the expression of *Hmox1*, could work in concert to limit the increase in *Spic* expression and the subsequent increase in *Gdf15* expression.

Spic$^{-/-}$ mice fail to increase *Gdf15* expression and initiate stress erythropoiesis in response to zymosan

Our data support a model wherein the heme-dependent increase in *Spic* expression is a central event in inducing stress erythropoiesis in response to inflammation. On the basis of these data, *Spic*$^{-/-}$ mice would be predicted to have a defect in inducing stress erythropoiesis. As reported previously, we observed fewer F4/80^{+} cells in the spleens of *Spic*$^{-/-}$ mice (Fig. 6A). Furthermore, the F4/80^{+} population in these mice also exhibited a significant decrease in phagocytosis of CFSE^{+} erythrocytes compared to wild-type mice 3 hours after inducing inflammation with zymosan (Fig. 6B). *Gdf15* expression was lower in F4/80^{+}CFSE^{+} cells in *Spic*$^{-/-}$ mice than in wild-type controls (Fig. 6C). The failure to increase *Gdf15* expression resulted in a defect in the expansion of the stress BFU-E population in the spleen. *Spic*$^{-/-}$ mice made fewer stress BFU-Es at 36 and 72 hours after zymosan than did wild-type mice (Fig. 6D). Our observation that *Spic*$^{-/-}$ F4/80^{+} cells in the spleen phagocytosed fewer CFSE^{+} erythrocytes suggested that SPI-C may also promote macrophage function. We generated BMDMs from wild-type and *Spic*$^{-/-}$ mice and treated them with zymosan in vitro. We observed no difference between wild-type and *Spic*$^{-/-}$ BMDMs in the decrease in surface levels of SIRPα (Fig. 6E). Furthermore, in contrast to what we observed in vivo, *Spic*$^{-/-}$ and wild-type BMDMs exhibited similar frequencies of erythrophagocytosis in response to zymosan, which is consistent with those events being upstream of *Spic* activation (Fig. 6F). However, the ability of zymosan to induce *Gdf15* expression in vitro was severely compromised in *Spic*$^{-/-}$ BMDMs (Fig. 6G).

To demonstrate the importance of *Spic* expression in splenic macrophages during inflammation-induced stress erythropoiesis, we tested the ability of wild-type monocytes to rescue inflammation-induced stress erythropoiesis in *Spic*$^{-/-}$ mice. Previous studies showed that heme-dependent activation of *Spic* drives the development of monocytes into red pulp macrophages (26, 28). We adoptively transferred purified CD11b^{+}Ly6G^{neg}Ly6C^{+} monocytes into either wild type or *Spic*$^{-/-}$ recipients (Fig. 6H). *Spic*$^{-/-}$ mice with wild-type donor monocytes exhibited a mild, but significant, increase in stress BFU-Es at 36 hours compared with *Spic*$^{-/-}$ mice receiving no donor cells (Fig. 6I). By 72 hours, however, *Spic*$^{-/-}$ mice with wild-type donor monocytes had numbers of stress BFU-Es similar to wild-type mice, indicating that *Spic* expression in monocytes and red pulp macrophages is critical for the induction of stress erythropoiesis by inflammatory signaling (Fig. 6I). *Gdf15*$^{-/-}$ mice have defective stress erythropoiesis but, unlike *Spic*$^{-/-}$ mice, have normal development of red pulp macrophages (47). To confirm that the absence of stress erythropoiesis in *Spic*$^{-/-}$ mice was due to the inability to induce GDF15 signaling in macrophages rather than a result of general red pulp macrophage dysfunction, *Gdf15*$^{-/-}$ monocytes were adoptively transferred into *Spic*$^{-/-}$ mice.

Gdf15$^{-/-}$ monocytes did not rescue BFU-E formation in *Spic*$^{-/-}$ mice (Fig. 6I). Donor cells comprised between 2 and 11% of recipient spleens at 72 hours after adoptive transfer, and there was no difference in the homing of donor cells to the spleen between wild-type, *Spic*$^{-/-}$, and *Gdf15*$^{-/-}$ mice (fig. S3A). Adoptive transfer of wild-type monocytes into *Gdf15*$^{-/-}$ mice resulted in a small increase in BFU-Es (fig. S3B). This partial rescue most likely reflects a role for *Gdf15* expression in SEPs, which would not be rescued by the control

monocyte transfers. Similar results were obtained when native phagocytes were depleted in *Spic*$^{-/-}$ and wild-type mice using clodronate liposomes and wild-type BMDMs were adoptively transferred into these macrophage-depleted recipients (fig. S3C). Transfer of wild-type BMDMs into *Spic*$^{-/-}$ mice resulted in a partial rescue with the number of stress BFU-Es being nearly equivalent to that in wild-type mice and increased compared to control *Spic*$^{-/-}$ mice that received no donor cells (fig. S3D). Together, these data support the conclusion that SPI-C-dependent expression of *Gdf15* in splenic macrophages is essential for the activation of stress erythropoiesis during inflammation.

TNF-α and IL-1β promote expansion and differentiation of SEPs

Activation of TLR2 by zymosan, in addition to increasing erythrophagocytosis, also induces the expression of genes encoding proinflammatory cytokines. Previous work by others showed that inflammation inhibits bone marrow steady-state erythropoiesis (5–13). This effect is in part due to proinflammatory cytokines, such as TNF-α and IFN-γ (5, 7–11). Furthermore, chronic exposure of HSCs to IL-1β results in activation of the transcription factor PU.1, which both drives myelopoiesis and represses erythropoiesis and lymphopoiesis (13). At 3 hours after treatment, zymosan induced an increase in *Tnfa, Il1b*, and *Ifng* mRNA expression in the spleen (Fig. 7, A, D, and G). We observed a significant increase in TNF-α^{+}F4/80^{+} and IL-1β^{+}F4/80^{+} cells by flow cytometry after treatment with zymosan (Fig. 7, B, C, E, and F). IFN-γ^{+}F4/80^{+} cells were detectable by flow cytometry but were not significantly changed compared with unstimulated controls (Fig. 7, H and I). The expansion of SEPs despite the presence of proinflammatory cytokines known to inhibit steady- state erythropoiesis further supports the idea that SEPs respond differently than steady-state erythroid progenitors to inflammatory signals.

To determine how exposure to proinflammatory cytokines affects SEPs in the spleen, we used a two-stage in vitro culture system developed in our laboratory that includes the signals necessary to promote the expansion and differentiation of stress progenitors (20). Unfractionated bone marrow cells were cultured in stress erythropoiesis expansion media (SEEM) and pulsed with TNF-α, IFN-γ, or IL-1β for 24 hours. Transient exposure to TNF-α had no effect on the expansion of SEPs compared to cells grown only in SEEM after 7 days of culture (Fig. 7J). However, treatment with IFN-γ significantly decreased cell expansion (Fig. 7J). IL-1β treatment also resulted in a moderate but insignificant decrease in cell expansion (Fig. 7K). SEPs expanded in SEEM exhibit limited differentiation potential (20). However, when cells were plated in SEEM only to quantify stress BFU-Es after 7 days, cells treated with either TNF-α or IL-1β showed a significant increase in the frequency of stress BFU-Es, indicating that the presence of IL-1β or TNF-α enhanced erythroid output (Fig. 7K). The increase in stress BFU-Es with TNF-α treatment was more profound when total numbers of stress BFU-Es per culture were calculated (Fig. 7L). The overall increase with IL-1β treatment was more modest because of the slight decrease in growth compared to untreated cells (Fig. 7L). Unlike its effect on steady-state erythropoiesis, IFN-γ not only seemed to inhibit the growth of SEPs but also had no significant effect on erythroid output because there was no significant change in stress BFU-Es (Fig. 7K). However, the number of stress BFU-Es in the total culture was lower because there were far fewer cells in cultures treated with IFN-γ (Fig. 7L). These data suggest that inflammation not only increases the

expression of *Gdf15* and *Bmp4* to induce stress erythropoiesis but also, through the action of the proinflammatory cytokines TNF-α and IL-1β, further promotes stress erythropoiesis by expanding the population of SEPs in the spleen.

DISCUSSION

Our results indicate that inflammatory stimuli, such as zymosan and proinflammatory cytokines, increase the phagocytosis of circulating erythrocytes, and this drives changes in gene expression in splenic macrophages, which then activate the BMP4-dependent stress erythropoiesis pathway. Previous studies demonstrated an expansion of the erythroid compartment in the spleen during other models of infection and inflammation (23–25). However, most of these studies were performed after the establishment of AI and several days to weeks after the initial infection or inflammatory stimulus. Here, we demonstrate that there was a rapid stress erythroid response after the initial inflammatory stimulus that occurred before the onset of anemia. Stress erythropoiesis is typically considered a stress response to acute anemic or hypoxic stress. However, our data show that inflammation rapidly induced stress erythropoiesis before any overt anemia or tissue hypoxia. We propose that inflammation induces stress erythropoiesis to maintain erythroid homeostasis. Proinflammatory cytokines inhibit bone marrow erythropoiesis by shifting bone marrow hematopoiesis to favor myelopoiesis to generate innate effector cells, which are critical to resolve inflammation and clear pathogens during infection, at the expense of erythropoiesis. The ability of inflammation to induce stress erythropoiesis ensures that sufficient erythrocytes will be produced to maintain tissue oxygenation during infection. This temporary shift to extramedullary erythropoiesis is needed until homeostatic conditions in the bone marrow can be reestablished.

Our data also outline a previously unknown mechanism for the activation of the stress erythropoiesis pathway under inflammatory conditions (Fig. 7M). Stimulation of TLRs increases the phagocytosis of circulating erythrocytes, which is critical in the activation of stress erythropoiesis. Our data show that small changes in the amount of SIRPα on the surface of splenic macrophages coupled with TLR signaling was sufficient to increase erythrophagocytosis. The breakdown of hemoglobin and the subsequent increase in intracellular heme led to changes in the expression of several heme-regulated genes and decreased the abundance of BACH1 protein. Turnover of BACH1 derepressed *Spic* expression, leading to increased expression of its downstream target *Gdf15*.

Previous work by Bian *et al.* showed that the CD47-SIRPα signaling axis suppresses erythrophagocytosis. Mice mutant for either CD47 or SIRPα exhibit exaggerated responses to inflammatory stimuli, which requires PI3K- and Syk-dependent signaling downstream of TLRs to induce phagocytosis of erythrocytes. This increased turnover leads to anemia and splenomegaly (42). Similarly, our data show that zymosan reduced the abundance of SIRPα on splenic macrophages, which, in combination with activation of the PI3K and Syk signaling pathways, drove increased erythrocyte turnover and induction of *Spic* and *Gdf15* expression. TLR signaling can also increase the surface abundance of calreticulin (CRT), which can induce phagocytosis of cells (48). Although we did observe an increase in surface CRT after zymosan treatment, that increase was not substantial and CRT-dependent

phagocytosis relies on Bruton's tyrosine kinase–dependent signaling, not PI3K and Syk signaling.

Erythrophagocytosis appears to be a general mechanism by which stress erythropoiesis is induced. Liao *et al.* observed increased erythrocyte uptake by red pulp macrophages and monocytes recruited into the spleen during the first 4 days after bone marrow transplant (38). Macrophages that phagocytosed erythrocytes produced CCL2, a chemokine that recruits monocytes to the spleen to contribute to the developing stress erythropoiesis niche. In addition, increased *Spic* expression is observed in the developing splenic niche, which corresponds with an increase in *Gdf15* and *Bmp4* expression (38). These data support a role for the heme-dependent increase in expression of *Spic* to stimulate the activation of stress erythropoiesis by inducing expression of *Gdf15* and subsequently the expression of *Bmp4*. The induction of *Gdf15* is a key initiating signal in the activation of stress erythropoiesis. Others have shown that *Gdf15* expression is directly regulated by NF-κB. However, although our data indicate that TLR-dependent signaling plays a role in stimulating *Gdf15* expression, it did not require NF-κB. It remains unclear whether SPI-C and TLR signaling events promote *Gdf15* expression directly or indirectly, and future studies are needed to fully understand this interaction.

In addition to eliciting changes in erythrophagocytosis, proinflammatory cytokines are induced by inflammation. Our data also clearly demonstrate that SEPs are not affected by proinflammatory cytokines in the same way as are steady-state erythroid progenitors. Many studies have demonstrated the direct and indirect inhibition of erythroid progenitors by TNF-α, IFN-γ, and IL-1β (2, 5–11, 13, 49). Both IFN-γ and IL-1β signaling drive cells toward the myeloid lineage (13, 50). TNF-α and IFN-γ have been shown to inhibit the proliferation and differentiation of erythroid progenitors in the marrow (5, 7–11). A study examining stress erythropoiesis during inflammatory conditions showed that IFN-γ did not affect stress BFU-Es in the spleen, whereas it negatively affected numbers of BFU-Es in the bone marrow (26). Our data shows that TNF-α and, to a lesser extent, IL-1β enhanced the erythroid potential of bone marrow cells cultured under stress erythropoiesis conditions, which supports a model wherein acute exposure to TNF-α and IL-1β acts in concert with other stress erythropoiesis signals to promote the expansion of erythroid progenitors during inflammation. It is unclear whether TNF-α and IL-1β are acting on SEPs directly or affecting them indirectly through macrophages, and more work will be necessary to fully understand the relationship between SEPs and these proinflammatory cytokines. These data provide new insights into the complex interactions of SEPs with the splenic microenvironment and the unique signals that affect their proliferation and differentiation.

Our analysis used a model of sterile inflammation that combined LPS and zymosan stimulation. However, our observation that deletion of MyD88 blocked the increase in erythrophagocytosis and the induction of stress erythropoiesis suggests that this response would be induced by activation of many different pattern recognition receptors that stimulate MyD88-dependent signaling. These data also provide an explanation as to why *Salmonella* infection induces the expansion of splenic erythroid progenitors and suggest that changes in myelopoiesis during infection may require compensatory stress erythropoiesis in the spleen as well (24, 25).

Together, these data suggest a new paradigm for inflammatory responses that incorporate stress erythropoiesis. In this model, inflammatory responses can mobilize and expand innate immune effectors cells at the expense of steady-state erythropoiesis because these same signals also induce stress erythropoiesis to maintain homeostasis. Ideally, the inflammation is resolved in a timely manner, and erythrocyte numbers are maintained. Unfortunately, this system breaks down in chronic inflammatory disease. Stress erythropoiesis does not generate erythrocytes at a constant rate but rather generates waves of new erythrocytes with a periodicity of about 28 days. Increased erythrocyte turnover coupled with inhibition of steady-state erythropoiesis erodes the increase in reticulocytes produced by stress erythropoiesis, resulting in anemia. If we follow the zymosan-treated mice for longer periods, we observe periodic anemia (fig. S4). These observations suggest that treatments geared to decreasing inflammation and boosting stress erythropoiesis may be effective in treating chronic AI.

MATERIALS AND METHODS

Mice

C57BL/6 mice were purchased from Taconic Biosciences Inc. All mice were 6 to 12 weeks old. *Gdf15*$^{-/-}$ mice were provided by S.-J. Lee at Johns Hopkins (51). *Spic*$^{-/-}$ mice were provided by K. Murphy at the Washington University School of Medicine (St. Louis, MO) (37). B6.129P2(SJL)-MyD88$^{tm1.1Defr}$/J mice were purchased from the Jackson Laboratory (44). Mouse strains were crossed to C57BL/6 mice and maintained on that background before use. All procedures were approved by the Institutional Animal Care and Use Committee of the Pennsylvania State University.

Zymosan-induced generalized inflammation

Mice were first treated with 40 μg of LPS from *Escherichia coli* 0128:B12 (L2887, Sigma-Aldrich) at a concentration of 200 μg/ml, and this was followed 6 days later by zymosan A from *Saccharomyces cerevisiae* (Z4250, Sigma-Aldrich) at a concentration of 0.48 mg/g mouse. All treatments were administered by intraperitoneal injection.

Murine cell cultures

Murine bone marrow was isolated from the femurs and cultured in SEEM for 7 days at normoxia as previously described and plated for colony assays (20). Briefly, SEEM is composed of Iscove's modified Dulbecco's media containing 10% fetal bovine serum, insulin (10 μg/ml), holo-transferrin (200 μg/ml), 2 mM L-glutamine, ciprofloxacin (10 μg/ml), 1% bovine serum albumin (BSA), 2-mercaptoethanol (7 μl/liter), GDF15 (30 ng/ml, Biomatik), BMP4 (15 ng/ml, R&D Systems), sonic hedgehog (SHH) (25 ng/ml, GoldBio), and stem cell factor (SCF) (50 ng/ml, Gold-Bio). TNF-α (1330–01, GoldBio) was added to cultures for 24 hours at a concentration of 50 ng/ml. After 24 hours, cells were washed and replated with fresh SEEM.

Colony assays

Murine splenocytes or bone marrow were plated in methylcellulose media (M3334, Stem Cell Technologies) at a concentration of 1×10^5 cells per well in a 12-well tissue culture

plate. For bone marrow, IL-3 (25 ng/ml) and EPO (3 U/ml) were added to methylcellulose media, and cells were incubated at 20% O_2 for 7 days before assessing BFU-Es. For splenocytes, BMP4 (15 ng/ml), SCF (50 ng/ml), SHH (25 ng/ml), GDF15 (15 ng/ml), and EPO (3 U/ml) were added to methylcellulose media to assay stress BFU-E formation. Cells were incubated at 1% O_2 for 5 days before counting BFU-Es. BFU-Es were stained with benzidine solution for counting.

mRNA isolation and gene expression analysis

Total RNA was isolated using TRIzol reagent (15596, Invitrogen). Complementary DNA (cDNA) was generated using the high-capacity cDNA synthesis kit (Applied Biosystems). Quantitative reverse transcription polymerase chain reaction (PCR) was carried out using TaqMan probes and an ABI7300 real-time PCR system. TaqMan probes: *Bmp4* (Mm00432087_m1), *Gdf15* (Mm00442228_m1), *Epo* (Mm01202755_m1), *Spic* (Mm00488428_m1), *Flvcr* (Mm01320423_m1), *Hmox1* (Mm00516005_m1), *Tnfa* (Mm00443258_m1), and *18S* (Hs99999901_s1).

Western blotting

Primary antibodies recognizing HIF-2α (working concentration, 1:500; NB100–122, Novus Biologicals), BACH1 (working concentration, 1:1000; AF5777, R&D Systems), and β-actin (working concentration, 1:3000; MAB8929, R&D Systems) were used for Western blots. Secondary antibodies against rabbit (working concentration, 1:10,000; SC-2004, Santa Cruz Biotechnology) and goat (working concentration, 1:10,000; SC-2768, Santa Cruz Biotechnology) conjugated to horseradish peroxidase were used. Bands were visualized using Amersham ECL prime Western blotting detection reagent (working concentration, 1:10,000; RPN2106, GE Healthcare).

Enzyme-linked immunosorbent assays

Serum concentrations of EPO were determined using the commercially available mouse Erythropoietin Quantikine ELISA kit (MEP00B, R&D Systems) according to the manufacturer's instructions.

Flow cytometry

Flow cytometry was performed using a BD Accuri C6 flow cytometer (BD Biosciences), and data were analyzed in FlowJo v10. Cells were sorted on a Beckman Coulter MoFlo Astrios. Flow antibodies: c-Kit Alexa Fluor 647 (clone 2B8, 105818, BioLegend), Sca-1 phycoerythrin (PE)-Cy7 (clone D7, BDB558162, BD Biosciences), Ter119 PE (clone Ter119, BDB553673, BD Biosciences), CD71 FITC (fluorescein isothiocyanate) (clone C2, BDB553266, BD Biosciences), F4/80 PE-Cy7 (clone BM8, 123112, BioLegend), CD172a allophycocyanin (APC) (clone P84, BDB560106, BD Biosciences), FITC TNF-α (506304, BD Biosciences), FITC IL-1β (IC4013F, R&D Systems), and APC IFN-γ (505809, BioLegend). Working concentration for all flow cytometry antibodies was 1:200. For reticulocytes, whole blood was stained with thiazole orange (390062, Sigma-Aldrich) at room temperature for 1 hour and then analyzed by flow cytometry.

In vivo biotinylation of erythrocytes

Biotinylation was performed as previously described (39). In short, 1 mg of Biotin-X-NHS (Cayman Chemicals) was dissolved in 20 μl of dimethylformamide and diluted in PBS. Biotin was administered intravenously daily for three consecutive days. Biotinylated erythrocytes were quantified by flow cytometry using a Strepavidin-Pe-Cy7–conjugated antibody (working concentration 1:200; 557598, BD Biosciences).

In vivo transfusion assay

Erythrocytes were isolated by terminal cardiac puncture and labeled with CFSE (C34554, Life Technologies). About 200 μl of blood was removed from recipients by retro-orbital bleeding, and recipients were then transfused with labeled erythrocytes (total volume of 200 μl). Mice were treated with either zymosan or PBS 24 hours after transfusion. Splenic macrophages were examined by flow cytometry to determine levels of internalized CFSE-labeled erythrocytes.

In vitro erythrophagocytosis assay

BMDMs were grown in 20% L929-conditioned media for 7 days and then were replated at a density of 2×10^6 cells per well. BMDMs were stimulated overnight with zymosan (10 μg/ml) and LPS (10 ng/ml). RBCs were collected in an EDTA-coated tube, labeled with CFSE, and aged in Hepes buffer [10 mM Hepes, 140 mM NaCl, and 0.1% BSA (pH 7.4)] containing calcium (2.5 mM) and $Ca2^+$ ionophore (0.5 μM, A23187). RBCs were aged for 16 hours at 37°C. BMDMs were washed twice with PBS before aged RBCs were added at a concentration of 3×10^7 cells/ml (52). BMDMs were incubated with either 20 μM LY294002 (S1105, Selleckchem) or 100 μM piceatannol (S3026, Selleckchem) for 1 hour before the addition of aged RBCs. BMDMs were incubated with RBCs at 37°C for 1 hour and were then washed twice with PBS. BMDMs were harvested, and phagocytosis was assessed by flow cytometry. For in vitro phagocytosis assays using primary phagocytes, splenocytes were isolated and rested for 4 hours to allow cells to adhere. Cells were incubated with 30 μM JSH-23 (S7351, Selleckchem) for 4 hours while resting. Primary cells were then incubated with aged RBCs for 3 hours, and RNA was isolated.

Adoptive transfer of BMDMs and monocytes

Native phagocytes were depleted with clodronate liposomes (ClodronateLiposomes.org), which were administered for three consecutive days, and mice received 200 μl of clodronate liposomes (about 50 mg per mouse) according to the manufacturer's instructions. BMDMs (1×10^6) were adoptively transferred 24 hours after completion of clodronate treatment, and LPS was given the next day. Mice were treated with zymosan as described above. Monocytes were purified using the EasySep Monocyte Enrichment Kit from Stem Cell Technologies (19761) according to the manufacturer's instructions. Monocytes (1×10^6) were transferred into recipient mice, and zymosan was administered simultaneously.

Statistics

P values were determined using the Student's *t* test (two tailed), one-way analysis of variance (ANOVA) with either Dunnett's (when comparing to control) or Tukey's (for

pairwise comparisons) post-test, two-way ANOVA with Bonferroni post-test, or Mantel-Cox test. Significance was assigned when $P < 0.05$. Statistical analysis was performed using GraphPad Prism v7.03 software.

Supplementary Material

Refer to Web version on PubMed Central for supplementary material.

Acknowledgments:

We thank the members of the Paulson, Hankey-Giblin, and Prabhu laboratories for help and comments on the work. We thank N. Altman for help with statistical analysis. We thank S. Neering at the Huck Institutes Flow Cytometry Core Facility for help with the analysis.

Funding: L.F.B. was funded by a T32 Training Grant for Animal Models of Inflammation (award number 5T32AI074551-05). Research reported in this publication was supported by the National Center for Advancing Translational Sciences of the National Institutes of Health Award number TL1TR002016 (to M.D.Q.). The content is solely the responsibility of the authors and does not necessarily represent the official views of the NIH. This work was also funded by NIH R01 DK080040 (to R.F.P.), NIH R01 DK097865 (to M.V.-K.), NIH RO1 DK077152 (to K.S.P.), and USDA-NIFA Hatch project numbers PEN04581 [accession number 1005468 (to R.F.P. and P.H.-G.)] and PEN04605 (accession number 1010021 (to K.S.P.)].

REFERENCES AND NOTES

1. Jurado RL, Iron, infections, and anemia of inflammation. Clin. Infect. Dis 25, 888–895, (1997). [PubMed: 9356804]
2. Prakash D, Anemia in the ICU: Anemia of chronic disease vesus anemia of acute illness. Crit. Care Clin 28, 333–343 (2012). [PubMed: 22713609]
3. Sankaran VG, Weiss MJ, Anemia: Progress in molecular mechanisms and therapies. Nat. Med 21, 221–230 (2015). [PubMed: 25742458]
4. Weiss G, Ganz T, Goodnough LT, Anemia of inflammation. Blood 133, 40–50 (2019). [PubMed: 30401705]
5. Libregts SF, Gutiérrez L, de Bruin AM, Wensveen FM, Papadopoulos P, van Ijcken W, Ozgur Z, Philipsen S, Nolte MA, Chronic IFN-γ production in mice induces anemia by reducing erythrocyte life span and inhibiting erythropoiesis through an IRF-1/PU.1 axis. Blood 118, 2578–2588 (2011). [PubMed: 21725055]
6. Maciejewski J, Selleri C, Anderson S, Young NS, Fas antigen expression on CD34+ human marrow cells is induced by interferon gamma and tumor necrosis factor alpha and potentiates cytokine-mediated hematopoietic suppression in vitro. Blood 85, 3183–3190 (1995). [PubMed: 7538820]
7. Papadaki HA, Kritikos HD, Valatas V, Boumpas DT, Eliopoulos GD, Anemia of chronic disease in rheumatoid arthritis is associated with increased apoptosis of bone marrow erythroid cells: Improvement following anti-tumor necrosis factor-α antibody therapy. Blood 100, 474–482 (2002). [PubMed: 12091338]
8. Rusten LS, Jacobsen SE, Tumor necrosis factor (TNF)–alpha directly inhibits human erythropoiesis in vitro: Role of p55 and p75 TNF receptors. Blood 85, 989–996 (1995). [PubMed: 7849320]
9. Tsopra OA, Ziros PG, Lagadinou ED, Symeonidis A, Kouraklis-Symeonidis A, Thanopoulou E, Angelopoulou MK, Vassilakopoulos TP, Pangalis GA, Zoumbos NC, Disease-related anemia in chronic lymphocytic leukemia is not due to intrinsic defects of erythroid precursors: A possible pathogenetic role for tumor necrosis factor-alpha. Acta Haematol 121, 187–195 (2009). [PubMed: 19468203]
10. Xiao W, Koizumi K, Nishio M, Endo T, Osawa M, Fujimoto K, Sato I, Sakai T, Koike T, Sawada K, Tumor necrosis factor-α inhibits generation of glycophorin A^+ cells by $CD34^+$ cells. Exp. Hematol 30, 1238–1247 (2002). [PubMed: 12423676]

11. Zamai L, Secchiero P, Pierpaoli S, Bassini A, Papa S, Alnemri ES, Guidotti L, Vitale M, Zauli G, TNF-related apoptosis-inducing ligand (TRAIL) as a negative regulator of normal human erythropoiesis. Blood 95, 3716–3724 (2000). [PubMed: 10845902]
12. Nagai Y, Garrett KP, Ohta S, Bahrun U, Kouro T, Akira S, Takatsu K, Kincade PW, Toll-like receptors on hematopoietic progenitor cells stimulate innate immune system replenishment. Immunity 24, 801–812 (2006). [PubMed: 16782035]
13. Pietras EM, Mirantes-Barbeito C, Fong S, Loeffler D, Kovtonyuk LV, Zhang S, Lakshminarasimhan R, Chin CP, Techner JM, Will B, Nerlov C, Steidl U, Manz MG, Schroeder T, Passegue E, Chronic interleukin-1 exposure drives haematopoietic stem cells towards precocious myeloid differentiation at the expense of self-renewal. Nat. Cell Biol 18, 607–618 (2016). [PubMed: 27111842]
14. Gardenghi S, Renaud TM, Meloni A, Casu C, Crielaard BJ, Bystrom LM, Greenberg-Kushnir N, Sasu BJ, Cooke KS, Rivella S, Distinct roles for hepcidin and interleukin-6 in the recovery from anemia in mice injected with heat-killed Brucella abortus. Blood 123, 1137–1145 (2014). [PubMed: 24357729]
15. Nemeth E, Rivera S, Gabayan V, Keller C, Taudorf S, Pedersen BK, Ganz T, IL-6 mediates hypoferremia of inflammation by inducing the synthesis of the iron regulatory hormone hepcidin. J. Clin. Invest 113, 1271–1276 (2004). [PubMed: 15124018]
16. Harandi OF, Hedge S, Wu DC, McKeone D, Paulson RF, Murine erythroid short-term radioprotection requires a BMP4-dependent, self-renewing population of stress erythroid progenitors. J. Clin. Invest 120, 4507–4519 (2010). [PubMed: 21060151]
17. Lenox LE, Perry JM, Paulson RF, BMP4 and Madh5 regulate the erythroid response to acute anemia. Blood 105, 2741–2748 (2005). [PubMed: 15591122]
18. Perry JM, Harandi OF, Paulson RF, BMP4, SCF, and hypoxia cooperatively regulate the expansion of murine stress erythroid progenitors. Blood 109, 4494–4502 (2007). [PubMed: 17284534]
19. Perry JM, Harandi OF, Porayette P, Hegde S, Kannan AK, Paulson RF, Maintenance of the BMP4-dependent stress erythropoiesis pathway in the murine spleen requires hedgehog signaling. Blood 113, 911–918 (2009). [PubMed: 18927434]
20. Xiang J, Wu DC, Chen Y, Paulson RF, In vitro culture of stress erythroid progenitors identifies distinct progenitor populations and analogous human progenitors. Blood 125, 1803–1812 (2015). [PubMed: 25608563]
21. Kim A, Fung E, Parikh SG, Valore EV, Gabayan V, Nemeth E, Ganz T, A mouse model of anemia of inflammation: Complex pathogenesis with partial dependence on hepcidin. Blood 123, 1129–1136 (2014). [PubMed: 24357728]
22. Sasu BJ, Cooke KS, Arvedson TL, Plewa C, Ellison AR, Sheng J, Winters A, Juan T, Li H, Begley CG, Molineux G, Antihepcidin antibody treatment modulates iron metabolism and is effective in a mouse model of inflammation-induced anemia. Blood 115, 3616–3624 (2010). [PubMed: 20053755]
23. Achtman AH, Khan M, MacLennan IC, Langhorne J, Plasmodium chabaudi chabaudi infection in mice induces strong B cell responses and striking but temporary changes in splenic cell distribution. J. Immunol 171, 317–324 (2003). [PubMed: 12817013]
24. Hermida FP, Vieira DP, Fernandes ER, de Andrade HF Jr., Wave expansion of $CD34^{+}$ progenitor cells in the spleen in rodent malaria. Exp. Parasitol 121, 230–237 (2009). [PubMed: 19068215]
25. Jackson A, Nanton MR, O'Donnell H, Akue AD, McSorley SJ, Innate immune activation during Salmonella infection initiates extramedullary erythropoiesis and splenomegaly. J. Immunol 185, 6198–6204 (2010). [PubMed: 20952675]
26. Millot S, Andrieu V, Letteron P, Lyoumi S, Hurtado-Nedelec M, Karim Z, Thibaudeau O, Bennada S, Charrier JL, Lasocki S, Beaumont C, Erythropoietin stimulates spleen BMP4-dependent stress erythropoiesis and partially corrects anemia in a mouse model of generalized inflammation. Blood 116, 6072–6081 (2010). [PubMed: 20844235]
27. Wu DC, Paulson RF, Hypoxia regulates BMP4 expression in the murine spleen during the recovery from acute anemia. PLOS ONE 5, e11303 (2010).
28. Haldar M, Kohyama M, So AY, Kc W, Wu X, Briseno CG, Satpathy AT, Kretzer NM, Arase H, Rajasekaran NS, Wang L, Egawa T, Igarashi K, Baltimore D, Murphy TL, Murphy KM, Heme-

mediated SPI-C induction promotes monocyte differentiation into iron-recycling macrophages. Cell 156, 1223–1234 (2014). [PubMed: 24630724]

29. Volman TJ, Hendriks T, Goris RJ, Zymosan-induced generalized inflammation: Experimental studies into mechanisms leading to multiple organ dysfunction syndrome. Shock 23, 291–297 (2005). [PubMed: 15803050]
30. Hegde S, Lenox LE, Lariviere A, Porayette P, Perry JM, Yon M, Paulson RF, An intronic sequence mutated in flexed-tail mice regulates splicing of Smad5. Mamm. Genome 18, 852–860 (2007). [PubMed: 18060457]
31. Haase VH, Regulation of erythropoiesis by hypoxia-inducible factors. Blood Rev 27, 41–53 (2013). [PubMed: 23291219]
32. Maxwell PH, Wiesener MS, Chang GW, Clifford SC, Vaux EC, Cockman ME, Wykoff CC, Pugh CW, Maher ER, Ratcliffe PJ, The tumour suppressor protein VHL targets hypoxia-inducible factors for oxygen-dependent proteolysis. Nature 399, 271–275 (1999). [PubMed: 10353251]
33. Ratnam NM, Peterson JM, Talbert EE, Ladner KJ, Rajasekera PV, Schmidt CR, Dillhoff ME, Swanson BJ, Haverick E, Kladney RD, Williams TM, Leone GW, Wang DJ, Guttridge DC, NF-κB regulates GDF-15 to suppress macrophage surveillance during early tumor development. J. Clin. Invest 127, 3796–3809 (2017). [PubMed: 28891811]
34. Ogawa K, Sun J, Taketani S, Nakajima O, Nishitani C, Sassa S, Hayashi N, Yamamoto M, Shibahara S, Fujita H, Igarashi K, Heme mediates derepression of Maf recognition element through direct binding to transcription repressor Bach1. EMBOJ. 20, 2835–2843 (2001).
35. Suzuki H, Tashiro S, Hira S, Sun J, Yamazaki C, Zenke Y, Ikeda-Saito M, Yoshida M, Igarashi K, Heme regulates gene expression by triggering Crm1-dependent nuclear export of Bach1. EMBO J 23, 2544–2553 (2004). [PubMed: 15175654]
36. Zenke-Kawasaki Y, Dohi Y, Katoh Y, Ikura T, Ikura M, Asahara T, Tokunaga F, Iwai K, Igarashi K, Heme induces ubiquitination and degradation of the transcription factor Bach1. Mol. Cell. Biol 27, 6962–6971 (2007). [PubMed: 17682061]
37. Kohyama M, Ise W, Edelson BT, Wilker PR, Hildner K, Mejia C, Frazier WA, Murphy TL, Murphy KM, Role for Spi-C in the development of red pulp macrophages and splenic iron homeostasis. Nature 457, 318–321 (2009). [PubMed: 19037245]
38. Liao C, Prabhu KS, Paulson RF, Monocyte derived macrophages expand the murine stress erythropoietic niche during the recovery from anemia. Blood 132, 2580–2593 (2018). [PubMed: 30322871]
39. Khandelwal S, van Rooijen N, Saxena RK, Reduced expression of CD47 during murine red blood cell (RBC) senescence and its role in RBC clearance from the circulation. Transfusion 47, 1725–1732 (2007). [PubMed: 17725740]
40. Kong X-N, Yan H-X, Chen L, Dong L-W, Yang W, Liu Q, Yu L-X, Huang D-D, Liu S-Q, Liu H, Wu M-C, Wang H-Y, LPS-induced down-regulation of signal regulatory protein α contributes to innate immune activation in macrophages. J. Exp. Med 204, 2719–2731 (2007). [PubMed: 17954568]
41. Li LX, Atif SM, Schmiel SE, Lee SJ, McSorley SJ, Increased susceptibility to Salmonella infection in signal regulatory protein a-deficient mice. J. Immunol 189, 2537–2544 (2012). [PubMed: 22851710]
42. Bian Z, Shi L, Guo YL, Lv Z, Tang C, Niu S, Tremblay A, Venkataramani M, Culpepper C, Li L, Zhou Z, Mansour A, Zhang Y, Gewirtz A, Kidder K, Zen K, Liu Y, Cd47-Sirpa interaction and IL-10 constrain inflammation-induced macrophage phagocytosis of healthy self-cells. Proc. Natl. Acad. Sci. U.S.A 113, E5434–E5443 (2016).
43. Quigley JG, Yang Z, Worthington MT, Phillips JD, Sabo KM, Sabath DE, Berg CL, Sassa S, Wood BL, Abkowitz JL, Identification of a human heme exporter that is essential for erythropoiesis. Cell 118, 757–766 (2004). [PubMed: 15369674]
44. Adachi O, Kawai T, Takeda K, Matsumoto M, Tsutsui H, Sakagami M, Nakanishi K, Akira S, Targeted disruption of the MyD88 gene results in loss of IL-1- and IL-18-mediated function. Immunity 9, 143–150 (1998). [PubMed: 9697844]
45. Kaisho T, Akira S, Toll-like receptor function and signaling. J. Allergy Clin. Immunol 117, 979–987 (2006). [PubMed: 16675322]

46. Nairz M, Schroll A, Moschen AR, Sonnweber T, Theurl M, Theurl I, Taub N, Jamnig C, Neurauter D, Huber LA, Tilg H, Moser PL, Weiss G, Erythropoietin contrastingly affects bacterial infection and experimental colitis by inhibiting nuclear factor-κB-inducible immune pathways. Immunity 34, 61–74 (2011). [PubMed: 21256055]

47. Hao S, Xiang J, Wu DC, Fraser JW, Ruan B, Cai J, Patterson AD, Lai ZC, Paulson RF, Gdf15 regulates murine stress erythroid progenitor proliferation and the development of the stress erythropoiesis niche. Blood Adv 3, 2205–2217 (2019). [PubMed: 31324641]

48. Feng M, Chen JY, Weissman-Tsukamoto R, Volkmer JP, Ho PY, McKenna KM, Cheshier S, Zhang M, Guo N, Gip P, Mitra SS, Weissman IL, Macrophages eat cancer cells using their own calreticulin as a guide: roles of TLR and Btk. Proc. Natl. Acad. Sci. U.S.A 112, 2145–2150 (2015). [PubMed: 25646432]

49. Molica S, Mirabelli R, Molica M, Levato L, Mauro FR, Foà R, Clinical relevance and treatment of nonautoimmune anemia in chronic lymphocytic leukemia. Cancer Manag. Res 3, 211–217 (2011). [PubMed: 21792329]

50. Belyaev NN, Brown DE, Diaz AI, Rae A, Jarra W, Thompson J, Langhorne J, Potocnik AJ, Induction of an IL7-R^{+}c-Kit^{hi} myelolymphoid progenitor critically dependent on IFN-γ signaling during acute malaria. Nat. Immunol 11, 477–485 (2010). [PubMed: 20431620]

51. Hsiao EC, Koniaris LG, Zimmers-Koniaris T, Sebald SM, Huynh TV, Lee SJ, Characterization of growth-differentiation factor 15, a transforming growth factor β superfamily member induced following liver injury. Mol. Cell. Biol 20, 3742–3751 (2000). [PubMed: 10779363]

52. Delaby C, Pilard N, Hetet G, Driss F, Grandchamp B, Beaumont C, Canonne-Hergaux F, A physiological model to study iron recycling in macrophages. Exp. Cell Res 310, 43–53 (2005). [PubMed: 16095591]

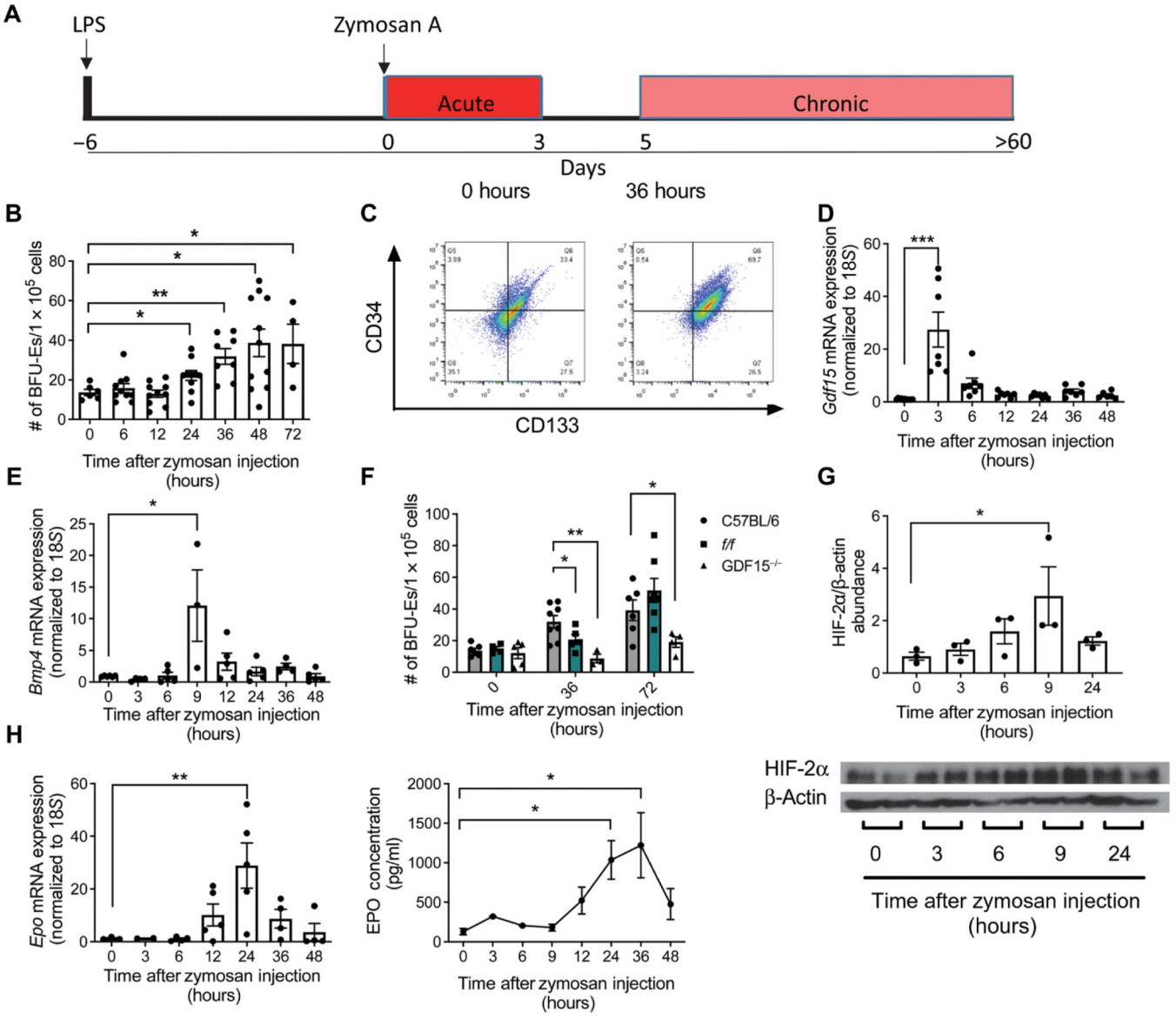

Fig. 1. Zymosan activates stress erythropoiesis by stimulating *Gdf15*, *Bmp4*, and *Epo* expression.

(**A**) Schematic of the LPS-zymosan model of sterile inflammation. (**B**) Splenocytes were harvested at the indicated time points and plated at a concentration of 1×10^5 cells per well in the presence of GDF15, BMP4, SCF, SHH, and EPO at low O_2 to induce the formation of stress BFU-Es. Stress BFU-Es were scored after 5 days by staining with benzidine. Data represent the mean ± SEM, one-way ANOVA with Dunnett's multiple comparison test, n = 4 to 11 mice per time point. (**C**) Flow cytometry analysis of splenocytes was performed at 0 and 36 hours after treatment with zymosan. Cells were gated on Kit^+ cells, and frequencies of $CD34^+$ and $CD133^+$ populations are shown in representative images. n = 3 to 5 mice per time point. (**D** and **E**) RNA was isolated from splenocytes at the indicated time points after zymosan injection, and relative expression of *Gdf15* and *Bmp4* compared to *18S* was determined by quantitative PCR. Data represent the mean ± SEM, one-way ANOVA with Dunnett's multiple comparison test, n = 3 to 10 mice per time point. (**F**) Splenocytes

harvested from mice at the indicated time points after zymosan treatment were plated under conditions to induce stress BFU-Es and stained with benzidine and counted after 5 days. Data represent the mean ± SEM, one-way ANOVA with Dunnett's multiple comparison test, $n = 3$ to 9 mice per time point. (**G**) Protein was isolated from kidneys at the indicated time points after zymosan treatment and Western blotted for HIF-2α and β-actin. HIF-2α abundance relative to β-actin was calculated using ImageJ. Data represent the mean ± SEM, one-way ANOVA with Dunnett's multiple comparison test, $n = 3$ mice per time point. (**H**) Quantification of *Epo* expression relative to *18S* in RNA isolated from kidneys and abundance of EPO in serum at the indicated time points after zymosan treatment. Data represent the mean ± SEM, one-way ANOVA with Dunnett's multiple comparison test, $n =$ 2 to 5 mice per time point (mRNA) and 2 to 8 mice per time point (protein). $^{*}P < 0.05$, $^{**}P < 0.01$, and $^{***}P < 0.005$.

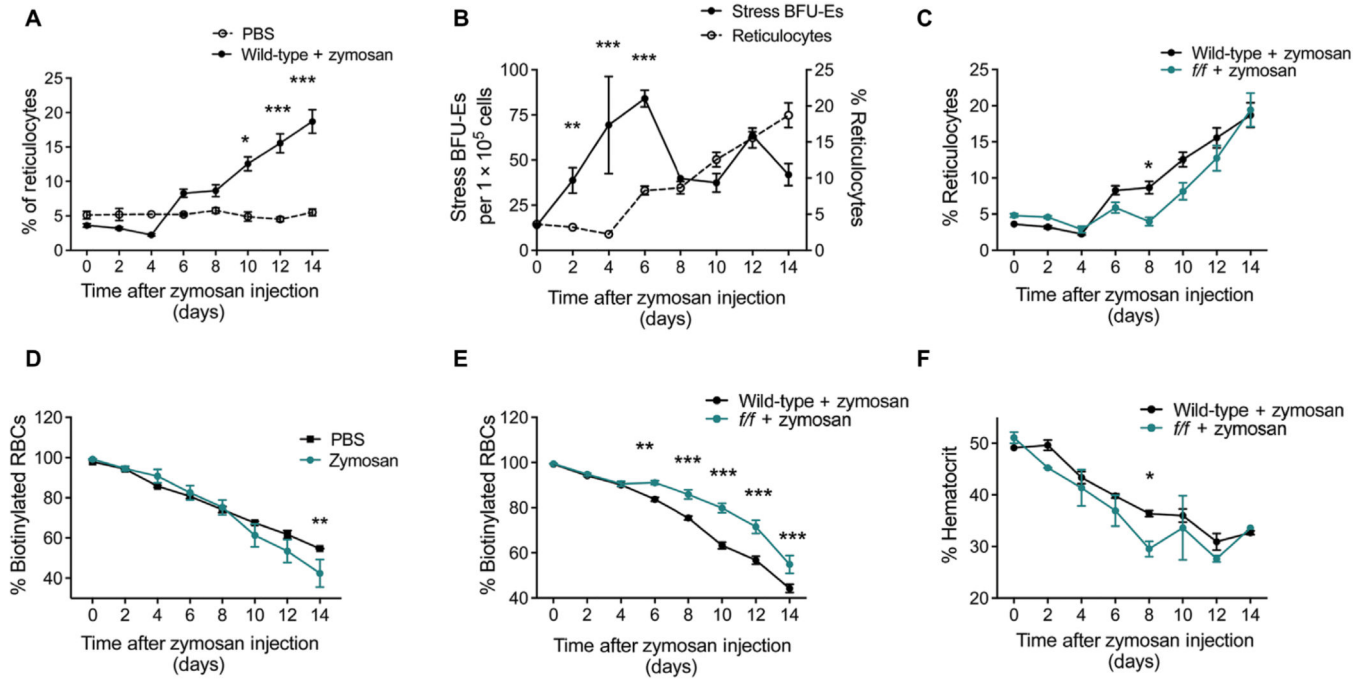

Fig. 2. Zymosan-induced inflammation results in an influx of new erythrocytes into circulation and lessens the severity of anemia.

(**A**) Wild-type (WT) mice were treated with either PBS or zymosan as described. The frequency of reticulocytes in the blood at the indicated time points was measured by flow cytometry after staining with thiazole orange. Data represent the mean ± SEM. Two-way ANOVA, $n = 4$ to 22 mice per group per time point. (**B**) Quantification of reticulocytes and stress BFU-Es after treatment with zymosan. Data were centered and scaled, and significance was determined using a two-way ANOVA, $n = 3$ to 22 mice per group per time point. (**C**) Quantification of reticulocytes in the blood of WT and *f/f* mice treated with zymosan as measured by flow cytometry after staining with thiazole orange. Data represent the mean ± SEM. Two-way ANOVA, $n = 10$ to 22 mice per group per time point. (**D** and **E**) Mice were injected with biotin for three consecutive days to label all circulating erythrocytes before treatment with zymosan or PBS. Blood was collected every other day thereafter, and in vivo biotinylation was measured by flow cytometry. Data represent the mean ± SEM. Two-way ANOVA, $n = 4$ to 19 per group per time point. (**F**) Blood was collected in heparin-coated microcapillary tubes after zymosan treatment and spun to determine hematocrit values. Data represent the mean ± SEM. $n = 2$ to 10 mice per group per time point. *$P < 0.05$, **$P < 0.01$, and ***$P < 0.005$.

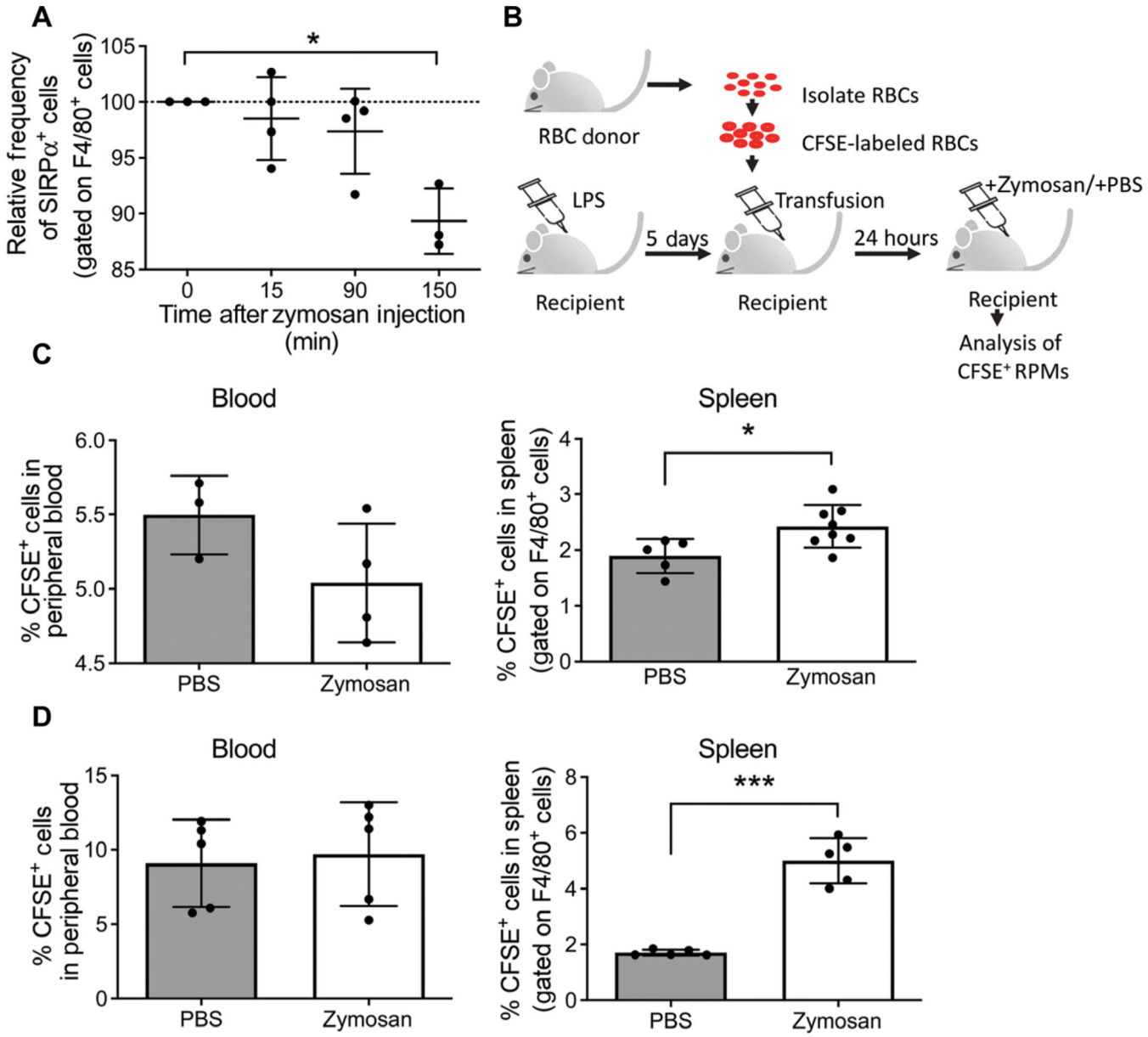

Fig. 3. Zymosan reduces Sirpα on the surface of macrophages and stimulates erythrophagocytosis.

(**A**) Splenocytes were isolated at the indicated time points after zymosan treatment, and the fraction of F4/80$^+$ cells (macrophages) that had Sirpα on the cell surface was measured by flow cytometry. Percentages of SIRPα$^+$ cells were normalized to 0 min for each experiment. Data represent the mean ± SEM, one-way ANOVA with Dunnett's multiple comparison test, n = 3 to 4 independent biological replicates. (**B**) Schematic depicting experimental design of CFSE$^+$ blood transfusion. RPM, red-pulp macrophage. (**C** and **D**) Quantification of CFSE$^+$ cells in blood and spleen from PBS- and zymosan-treated mice by flow cytometry at 3 hours (C) or 24 hours (D) after treatment. The spleen samples were gated on F4/80$^+$ cells (macrophages); F4/80$^+$ CFSE$^+$ cells represent macrophages that had phagocytosed CFSE$^+$

erythrocytes. Data represent the mean ± SEM, Student's *t* test, $n = 3$ to 8 mice per condition. $*P < 0.05$, $**P < 0.01$, and $***P < 0.005$.

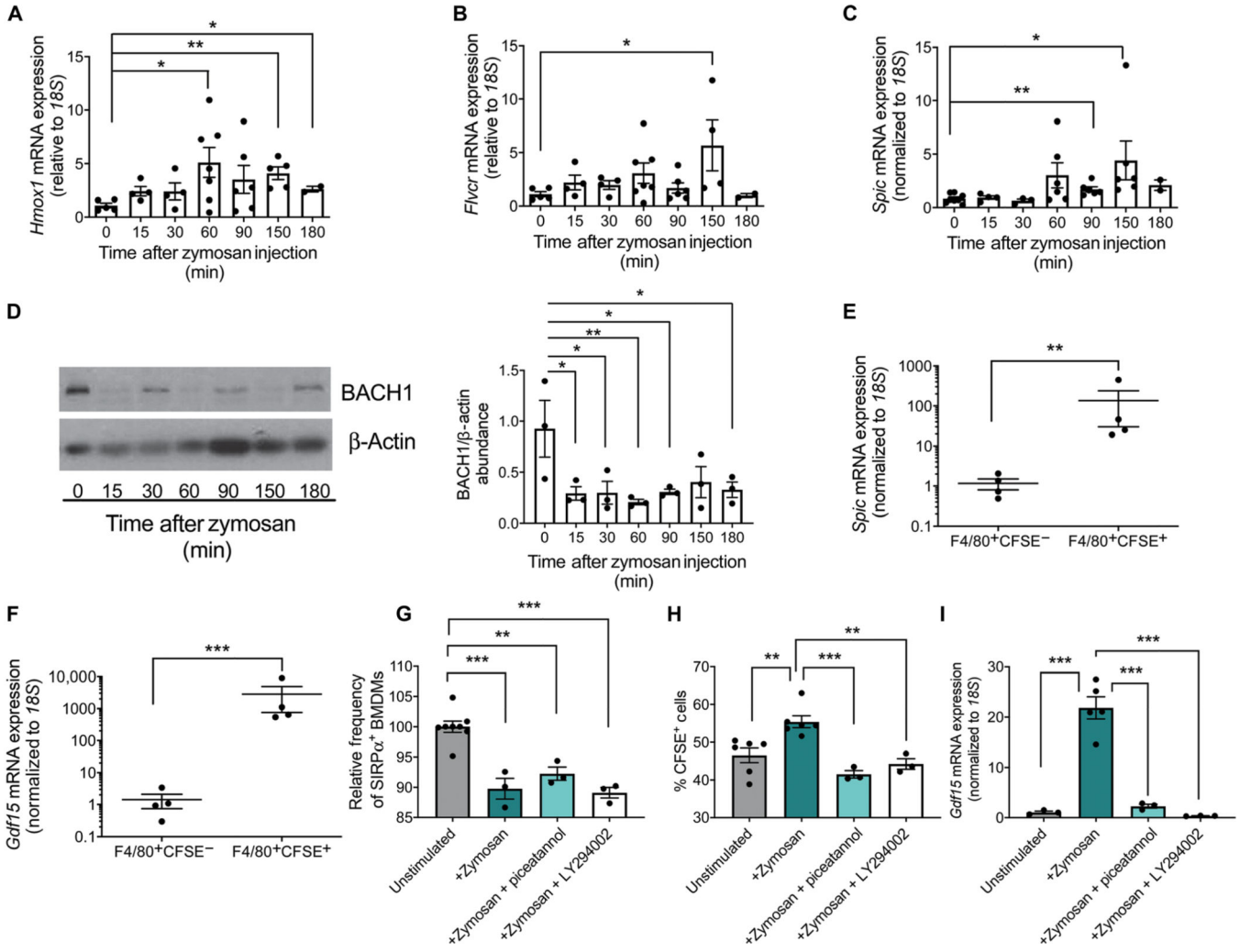

Fig. 4. Increased intracellular heme due to erythrophagocytosis drives changes in heme-dependent gene expression.

(**A to C**) RNA was isolated from splenocytes at the indicated times after zymosan treatment. The expression of *Hmox1* (A), *Flvcr* (B), and *Spic* (C) was measured relative to *18S*. Data represent the mean ± SEM, one-way ANOVA with Dunnett's multiple comparison test. n = 4 to 7 mice per time point (*Hmox1* and *Flvcr*); n = 3 to 8 mice per time point (*Spic*). (**D**) Representative Western blot and quantification of BACH1 abundance in the spleen at the indicated time points after zymosan treatment. β-Actin is included as a loading control and was used for calculating the relative abundance of BACH1 using ImageJ software. Data represent the mean ± SEM, one-way ANOVA with Dunnett's multiple comparison test, n = 3 mice per time point. (**E** and **F**) Splenocytes from mice transfused with CFSE-labeled erythrocytes were sorted into F4/80$^+$CFSE$^-$ and F4/80$^+$CFSE$^+$ populations 3 hours after zymosan treatment. Expression of *Spic* and *Gdf15* was measured relative to *18S* in RNA isolated from each population. Data represent the mean ± SEM. Student's t tests were performed on log scale–transformed data. n = 4 mice per group. (**G**) Quantification of the abundance of SIRPα on the surface of bone marrow–derived macrophages (BMDMs) relative to that on unstimulated BMDMs as measured by flow cytometry 1 hour after

zymosan treatment with or without the Syk inhibitor piceatannol or the PI3K inhibitor LY294002. All replicates were normalized to 0 min (baseline). Data represent the mean ± SEM. Data were analyzed by one-way ANOVA with Tukey's multiple comparison test, n = 3 to 6 independent biological replicates. (**H**) F4/80^{+}CFSE^{+} populations, representing phagocytosis of CFSE-labeled erythrocytes, were measured by flow cytometry 1 hour after the indicated treatments. Data represent the mean ± SEM. Data were analyzed by one-way ANOVA with Tukey's multiple comparison test, n = 3 to 6 independent biological replicates. (**I**) Quantification of *Gdf15* expression relative to *18S* in BMDMs 3 hours after the indicated treatments. Data represent the mean ± SEM. Data were analyzed by one-way ANOVA with Tukey's multiple comparison test, n = 3 to 6 independent biological replicates. *P < 0.05, **P < 0.01, and ***P < 0.005.

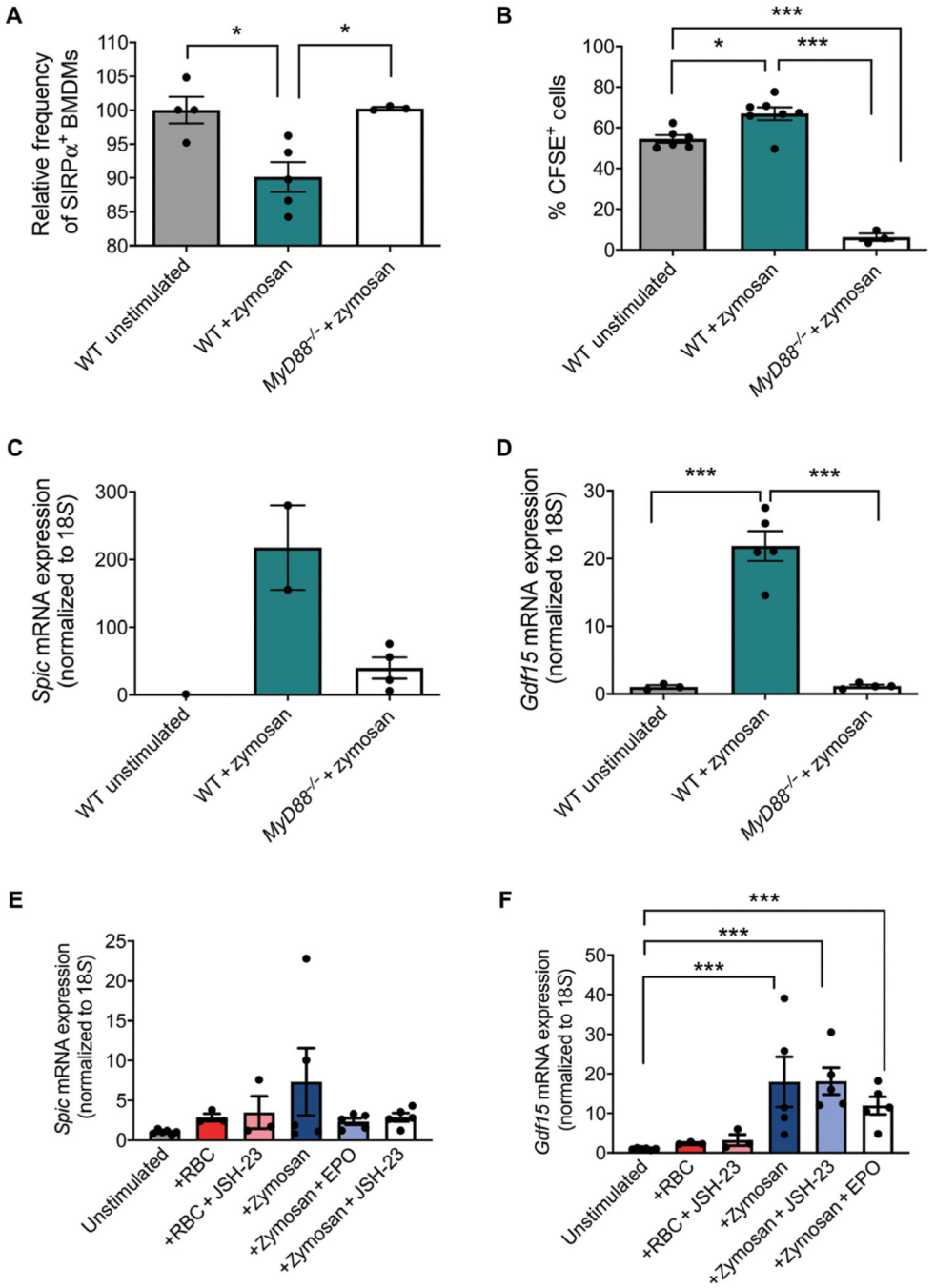

Fig. 5. Increased erythrophagocytosis and expression of *Spic* and *Gdf15* in response to zymosan depend on MyD88.

(**A**) BMDMs from WT and *MyD88*$^{-/-}$ mice were stimulated with LPS and zymosan for 3 hours, and the abundance of surface SIRPα was measured by flow cytometry. SIRPα abundances are indicated as percent of WT unstimulated cells. Data represent the mean ± SEM, one-way ANOVA with Tukey's multiple comparison test, $n = 3$ to 8 mice per genotype. (**B**) BMDMs from WT and *MyD88*$^{-/-}$ mice were stimulated for 12 hours and then incubated with CFSE-labeled erythrocytes for 1 hour. BMDMs were collected and analyzed

by flow cytometry for the presence of $CFSE^+$ cells. Data represent the mean ± SEM, one-way ANOVA with Tukey's multiple comparison test, $n = 3$ to 7 independent biological replicates. (**C** and **D**) Quantification of the expression of *Spic* (C) and *Gdf15* (D) relative to *18S* in from WT and $MyD88^{-/-}$ BMDMs. Data represent the mean ± SEM, one-way ANOVA with Tukey's multiple comparison test. $n = 2$ to 4 independent biological replicates (*Spic*), $n = 3$ to 7 independent biological replicates (*Gdf15*). (**E** and **F**) Quantification of the expression of *Spic* (E) and *Gdf15* (F) relative to *18S* in primary splenocytes incubated for 4 hours with or without JSH-23 to allow for adherence. Adherent cells were treated with zymosan and aged erythrocytes (RBC). Data represent the mean ± SEM. Data were analyzed by one-way ANOVA with Tukey's multiple comparison test on log scale-transformed data, $n = 3$ to 6 independent biological replicates. $^*P < 0.05$, $^{**}P < 0.01$, and $^{***}P < 0.005$.

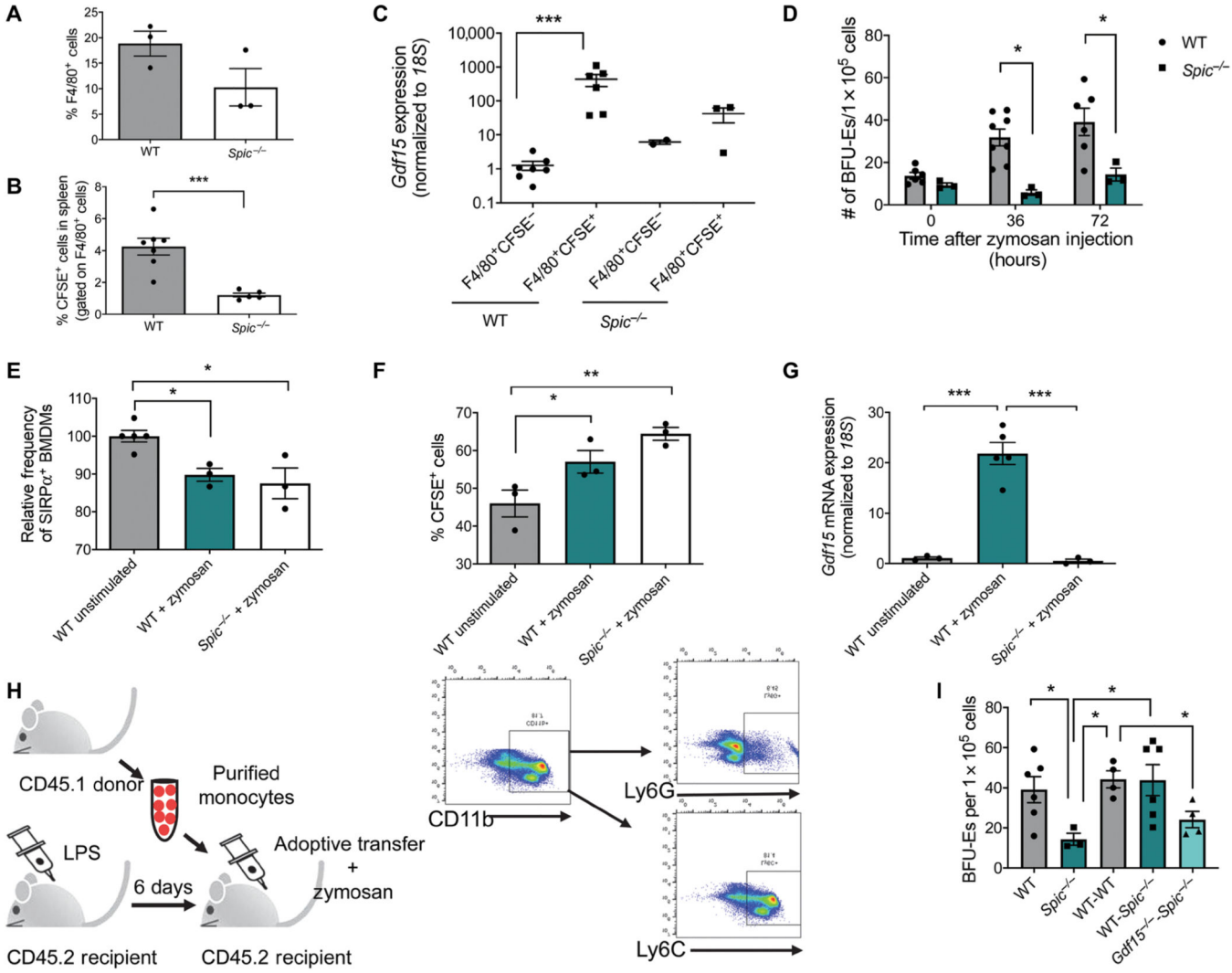

Fig. 6. SPI-C is critical for the induction of *Gdf15* and is required for the activation of stress erythropoiesis in response to inflammation.

(**A**) Percentage of F4/80$^+$ cells in the spleen as determined by flow cytometry. Data represent the mean ± SEM. Student's *t* test, $n = 3$ mice per genotype. (**B**) WT and *Spic*$^{-/-}$ mice were treated with LPS, transfused with CFSE-labeled erythrocytes, and treated with zymosan for 3 hours. The frequency of F4/80$^+$CFSE$^+$ cells in the spleen was determined by flow cytometry. Data represent the mean ± SEM. Student's *t* test, $n = 4$ to 7 mice per genotype. (**C**) Quantification of *Gdf15* relative to *18S* in F4/80$^+$CFSE$^-$ and F4/80$^+$CFSE$^+$ cells sorted from the spleen of *Spic*$^{-/-}$ or control mice. Data represent the mean ± SEM, one-way ANOVA with Tukey's multiple comparison test performed on log scale–transformed data, $n = 3$ to 7 mice per population for each genotype. (**D**) Splenocytes isolated from *Spic*$^{-/-}$ or control mice were isolated at the indicated times after zymosan treatment and cultured under conditions that induce stress erythropoiesis. Stress BFU-Es were scored by staining with benzidine. Data represent the mean ± SEM. Student's *t* test, $n = 3$ to 5 mice per genotype. (**E**) Relative frequencies of SIRPα$^+$ BMDMs after zymosan stimulation from *Spic*$^{-/-}$ and WT mice as measured by flow cytometry and normalized to WT unstimulated control. Data

represent the mean ± SEM, one-way ANOVA with Tukey's multiple comparison test, $n = 3$ to 5 independent biological replicates. (**F**) Percentage of $CFSE^+$ cells as measured by flow cytometry in zymosan-stimulated BMDMs 1 hour after the addition of CFSE-labeled erythrocytes. Data represent the mean ± SEM, one-way ANOVA with Dunnett's multiple comparison test, $n = 3$ independent biological replicates. (**G**) Quantification of *Gdf15* expression relative to *18S* in zymosan-stimulated BMDMs 3 hours after the addition of CFSE-labeled erythrocytes. Data represent the mean ± SEM, one-way ANOVA with Tukey's multiple comparison test, $n = 3$ to 5 independent biological replicates. (H) Schematic depicting experimental design of adoptive transfer of purified monocytes and representative flow cytometry plots demonstrating enrichment of the $CD11b^+Ly6G^-Ly6C^+$ monocyte population after magnetic bead selection. (**I**) Analysis of stress BFU-Es in the spleen after monocyte transfer at the indicated times after zymosan treatment. WT (WT mice receiving no monocytes); $Spic^{-/-}$ ($Spic^{-/-}$ mice receiving no monocytes); WT-WT (WT monocytes into WT mice); $WT\text{-}Spic^{-/-}$ (WT monocytes into $Spic^{-/-}$ mice); $Gdf15^{-/-}\text{-}Spic^{-/-}$ ($Gdf15^{-/-}$ monocytes into $Spic^{-/-}$ mice). Data represent the mean ± SEM, one-way ANOVA with Tukey's multiple comparison test, $n = 3$ to 6 mice per group. $^*P < 0.05$, $^{**}P < 0.01$, and $^{***}P < 0.005$.

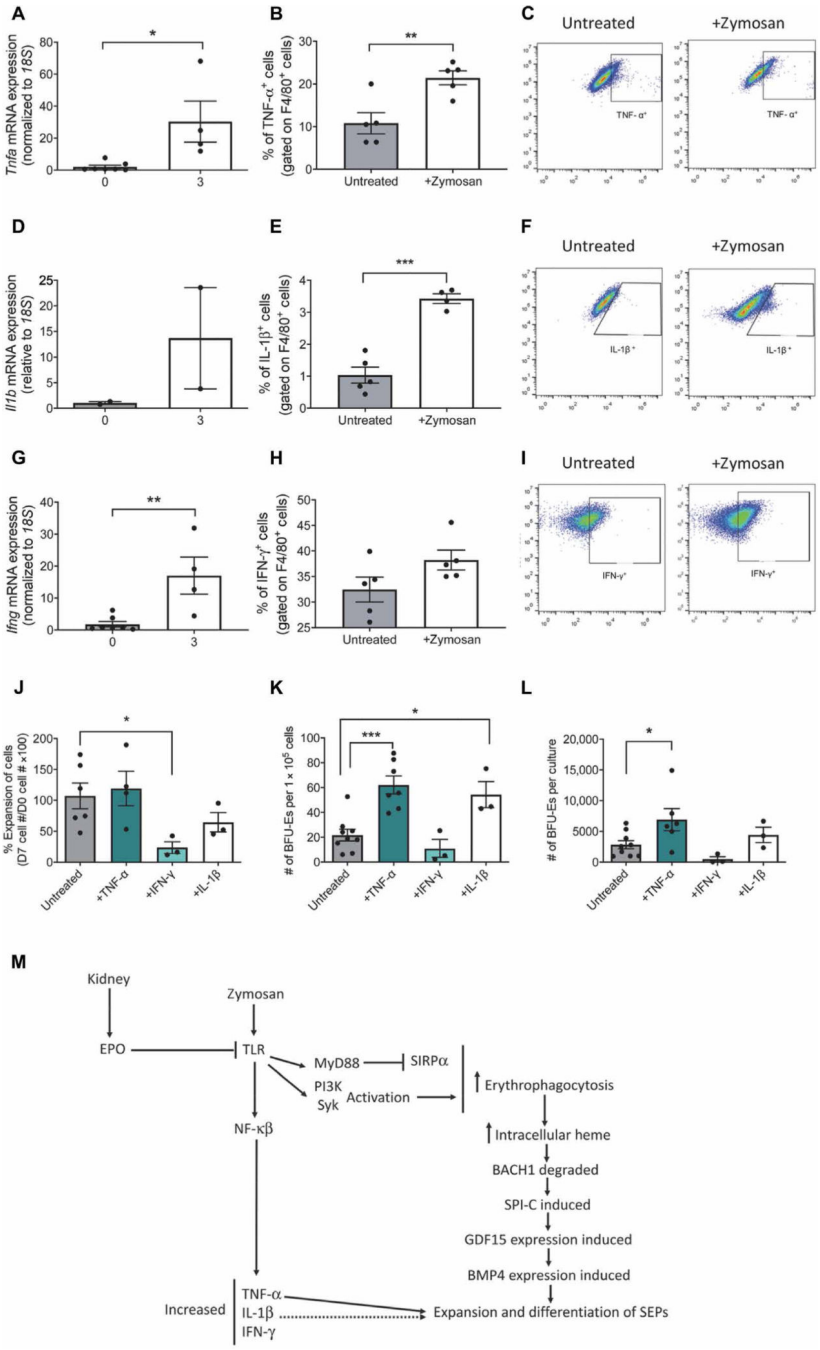

Fig. 7. TNF-α and IL-1β promote erythroid differentiation in vitro under stress erythropoiesis.

(**A to I**) Quantification of mRNA expression, percentage of F4/80$^+$ spleen cells positive for protein, and representative flow cytometry diagrams for TNF-α (A to C), IL-1β (D to F), and IFN-γ (G to I) in untreated and zymosan-treated mice. Data represent the mean ± SEM, Student's *t* test, $n = 4$ to 7 mice per group. (**J**) Percentage increase in number of bone marrow cells cultured with the indicated cytokines. Data represent the mean ± SEM, one-way ANOVA with Dunnett's multiple comparison test, n=3 to 8 independent biological replicates. (**K**) Frequency of stress BFU-Es generated after 7 days of culture with the

indicated cytokines. Data represent the mean ± SEM, one-way ANOVA with Dunnett's multiple comparison test, $n = 3$ to 8 independent biological replicates. (**L**) Total number of stress BFU-Es generated in cultures with the indicated cytokines. Data represent the mean ± SEM, one-way ANOVA with Dunnett's multiple comparison test, $n = 3$ to 8 independent biological replicates. (**M**) Schematic of the signaling events that occur during the activation of stress erythropoiesis in response to inflammation. *$P < 0.05$, **$P < 0.01$, and ***$P < 0.005$.